A Focusing Crystal von Hamos Spectrometer for X-ray Spectroscopy and X-ray Fluorescence Applications

Alexander P. Shevelko*[a], Alexander A. Antonov[a], Inna G.Grigorieva[a], Yury S. Kasyanov[a], Larry V. Knight[b], A. Reyes-Mena[c], Clark Turner[c], Quan Wang[b], Oleg F. Yakushev[a]

[a]P.N.Lebedev Physical Institute of the Russian Academy of Sciences, Leninsky Pr.53, Moscow 117924, Russia

[b]Department of Physics and Astronomy, Brigham Young University, Provo, UT 84602

[c]MOXTEK, Inc., 452 West 1260 North, Orem, UT 84057

ABSTRACT

The use of bent crystals with high integrated reflectivity in focusing crystal spectrometers (Johann and von Hamos schemes) is considered. It is shown that in a von Hamos scheme mosaic focusing takes place. Thus a mosaic crystal simultaneously provides high spectral resolution and high efficiency. Expressions for the mosaic focusing are obtained. Focusing mica and graphite crystal von Hamos spectrometers (radius of crystal curvature is 20 mm) are investigated: spectral and spatial resolution and absolute efficiency are measured in a spectral range of $2 - 2.6\mathring{A}$ using laser-produced plasma and iron isotope x-ray sources. The mica crystal spectrometer showed high spatial (up to 10 μm) and spectral ($\lambda/\delta\lambda \sim 1000$) resolution, whereas the graphite spectrometer showed very high efficiency ($30 - 70$ times higher than the mica crystal) and moderate spectral resolution ($\lambda/\delta\lambda \sim 500 - 750$). In the latter case mosaic focusing is observed: spectral resolution is $10 - 15$ times higher than spectral resolution determined by the mosaic spread of the crystal ($\lambda/\delta\lambda \sim 50$). The results allow one to estimate a maximum efficiency for focusing crystal spectrometers. Prospects for using the von Hamos spectrometers for x-ray spectroscopy and x-ray fluorescence are considered.

Keywords: bent crystals, x-ray spectroscopy, x-ray fluorescence

1. INTRODUCTION

High-efficiency crystal spectrometers require the use of crystals with high integrated reflectivity. The so-called mosaic crystals (pyrolytic graphite, LiF) show the highest integrated reflectivity. However, due to mosaic spread, these crystals have a wide rocking curve width that leads to a low spectral resolving power. For this reason, mosaic crystals are usually considered as high-sensitivity low-resolution diffracting devices. However, if mosaic crystals are used in a symmetrical scheme where a source of radiation and the image of the spectral lines are at equal distances from crystal planes, high resolution is achieved along with high sensitivity[1]. In this case, mosaic focusing in the direction of dispersion is observed: rays from a monochromatic point source are reflected off a mosaic crystal and converge to a point of equal distance to the crystal as the source. The geometry of mosaic focusing, which retains the high sensitivity of mosaic crystals without sacrificing spectral resolution, can be experimentally demonstrated[1]. It is very important to study the focusing schemes of crystal spectrometers, where high efficiency and high resolution can be achieved.

In this paper we study the use of mosaic crystals in focusing spectrometers (von Hamos and Johann schemes). For the von Hamos scheme, expressions for mosaic focusing are obtained for two cases: along and transverse to the dispersion direction. It is shown that in a von Hamos scheme mosaic focusing takes place only in the direction of dispersion whereas a mosaic crystal simultaneously provides high spectral resolution and efficiency. The focusing mica and graphite crystal von Hamos spectrometers (radius of crystal curvature is 20 mm) are investigated in a spectral range $2 - 2.6\mathring{A}$ using laser-produced plasma and iron isotope x-ray sources. The results show a maximum efficiency for focusing crystal spectrometers. This type of spectrometer is promising in x-ray fluorescence analysis and in x-ray spectroscopy of low-intensity sources.

*A.Shevelko: email: ashev@sci.lebedev.ru; Fax: +7-095-1352408/ 9382251; Telephone: +7-095-1326951

Advances in Laboratory-based X-Ray Sources and Optics, Carolyn A. MacDonald, Ali M. Khounsary, Editors, Proceedings of SPIE Vol. 4144 (2000) © 2000 SPIE · 0277-786X/00/$15.00

Downloaded From: http://proceedings.spiedigitallibrary.org/ on 03/27/2014 Terms of Use: http://spiedl.org/terms

2. VON HAMOS SPECTROMETER AND CRYSTAL SELECTION

In the von Hamos scheme[2,3], a crystal is bent into a cylindrical surface and the source and detector plane lie on the cylinder axis. In this case, monochromatic radiation from the source, after diffraction from the crystal arc, is focused to a point lying on the the spectrograph axis. Vertical focusing is used to take advantage of high spectrograph power. The spectra obtained with a von Hamos spectrograph form a two-dimensional image of the source for each wavelength. The abberations due to off-axis source point are limited so that spatial resolution cannot, in general, exceed the source size[1,4].

In the dispersion direction, a curved crystal in the von Hamos geometry works as a flat crystal. For a long crystal, the wavelength band $\Delta\lambda$ could be rather wide. For each wavelength in this band, the von Hamos geometry has a focusing property and, hence, high efficiency. Note that in other focusing schemes the wavelength band and efficiency are mutually exclusive factors[4]. In Johann and spherically bent crystal schemes, realization of maximum efficiency leads to a severe restriction of the recording wavelength band. Hence, the von Hamos scheme has the highest efficiency when spectra are recorded over a wide spectral range.

The relation between exposure I $[phot/cm^2]$ on the image plane and time integrated brightness of the monochromatic source L $[phot/cm^2 ster]$ is equal to[4]

$$I = B \cdot L \,. \tag{1}$$

The parameter $B[ster]$, is given by

$$B = \rho \cdot \vartheta \cdot \sin^2\theta \,, \tag{2}$$

defines the spectrograph efficiency (ρ is integral reflectivity, ϑ is angular aperture of the spectrometer, θ is the Bragg angle). It is easy to show that the ratio of efficiencies of the von Hamos spectrograph and a flat crystal spectrograph working at the same geometry is equal to[4]

$$R \cdot \vartheta / a \tag{3}$$

where a is source size. In the case of a laser-produced plasma ($a = 10 - 100\mu m$) at typical spectrograph parameters ($\vartheta \sim 1\ rad, R \sim 10\ mm$), this factor may be as large as $10^2 - 10^3$. This enhanced collecting efficiency of von Hamos spectrographs is very attractive for the development of x-ray spectroscopic diagnostics of low-intensity, small size sources. The increase of spectrometer efficiency requires the use of crystals with high integrated reflectivity ρ. However, due to mosaic spread, these crystals have a wide rocking curve width that leads to a low spectral resolving power:

$$\lambda/\delta\lambda = \tan\theta/\delta\theta \tag{4}$$

where $\delta\theta$ is rocking curve FWHM. Usually this value restricts the spectral resolving power in crystal spectrometers. Parameters of commonly used crystals are shown in Table 1. However, it is possible to compensate the mosaic spread of the crystal when the source and the detector are symmetrically disposed with respect to the diffracting planes[1].

Table 1. Parameters of some commonly used crystals

Crystal	*plane*	2*d*, Å	ρ, $10^{-5} rad$	$\delta\theta$, *min*	$\lambda/\delta\lambda = \tan\theta/\delta\theta$	*Ref.*
Mica	002	19.880	2-3	~ 2-4	~ 1,000-2,000	[5][6]
Quartz	1010	8.512	1-10	0.032-0.97	9,000-10,000	[6]
Graphite	002	6.696	60-200	41.4-87	24-200	[5, 6]
LiF	200	4.028	30-60	10-20	50-400	[5]

3. MOSAIC FOCUSING

The scheme of a von Hamos spectrometer is shown in Fig. 1. X-rays with wavelength λ are diffracted by the crystal according to the Bragg condition $2d\sin\theta = n\lambda$, where d, θ and n represent the crystal spacing between atomic layers, the angle of grazing incidence, and the order of diffraction, respectively. The distance x_0 from the source to the image for wavelength λ is $x_0 = 2R\cot\theta$, where R is the radius of curvature of the crystal.

Downloaded From: http://proceedings.spiedigitallibrary.org/ on 03/27/2014 Terms of Use: http://spiedl.org/terms

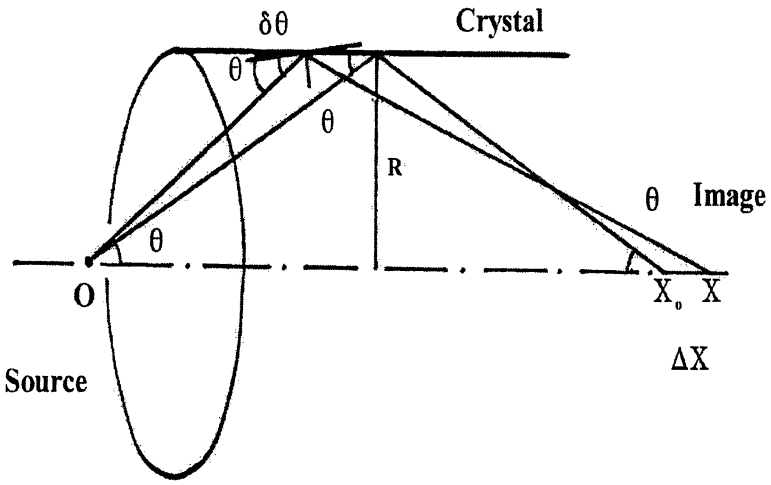


Figure 1. Ray path in a von Hamos spectrometer in direction of dispersion

On the surface of a mosaic crystal, we have well-ordered "crystallite" regions oriented within angle $\delta\theta$ (rocking curve width) with respect to the crystal surface. For any orientation $\delta\theta$ on the crystal surface where the Bragg condition is met, reflected rays intersect the spectrometer axis at a distance x which is very close to x_0. Let's find the difference $\Delta x = x - x_0$ using trigonometric formulae and assuming $\cot\theta \ll \cot\delta\theta$.

$$x_0 = 2R\cot\theta \tag{5}$$

$$x = R\cot(\theta+\delta\theta) + R\cot(\theta-\delta\theta) \tag{6}$$

$$\Delta x = 2R\cot\theta/\cot^2(\delta\theta) = 2R\cot\theta\tan^2(\delta\theta) \simeq 2R(\delta\theta)^2\cot\theta\,. \tag{7}$$

Note that the crystal section which reflects the same wavelength is small, i.e. symmetrical ray paths occur. Values of Δx at different angles θ when $\delta\theta = 0.5°$ (graphite crystal) and $R = 20\ mm$ are presented in Table 2. The corresponding spectral resolving power $\lambda/\delta\lambda = \lambda/\Delta x \cdot D$ is presented in the third column where D $[\mathring{A}/\mu m]$ is a linear dispersion. Spectral resolving power, defined by mosaic spread of the graphite crystal $\lambda/\delta\lambda = \tan\theta/\delta\theta$, is listed in the fourth column.

Table 2. Spectral resolution of graphite crystal

θ, *deg*	$\Delta x, \mu m$	$\lambda/\delta\lambda = \lambda/\Delta x \cdot D$	$\lambda/\delta\lambda = \tan\theta/\delta\theta$
10	17.30	6,500	20
20	8.40	13,400	42
40	3.60	31,000	96
80	0.54	208,000	652

It is clear from Table 2 that the mosaic spread of the crystal can be compensated. In this case, the spectrometer will have spectral resolution defined by the source size instead of the mosaic spread with the same integral reflectivity, i.e., mosaic focusing takes place.

In the plane which is perpendicular to the dispersion direction, mosaic focusing is absent (see Fig. 2). For the central ray we have the broadening $\Delta y = \delta\theta R/\sin\theta$ and $\Delta y = \delta\theta(R/\sin\theta)\cos\vartheta$ for the outer ray. Thus in this plane there is no mosaic focusing, and the von Hamos spectrometer does not have spatial resolution for sources with sizes

Downloaded From: http://proceedings.spiedigitallibrary.org/ on 03/27/2014 Terms of Use: http://spiedl.org/terms

less than Δy. For the Johann scheme, the symmetrical ray path is only for the central ray (see Fig. 3). There is no mosaic focusing at all except the Bragg angles $\theta \sim 90°$. This fact emphasizes the advantage of the von Hamos scheme when mosaic crystals are used.

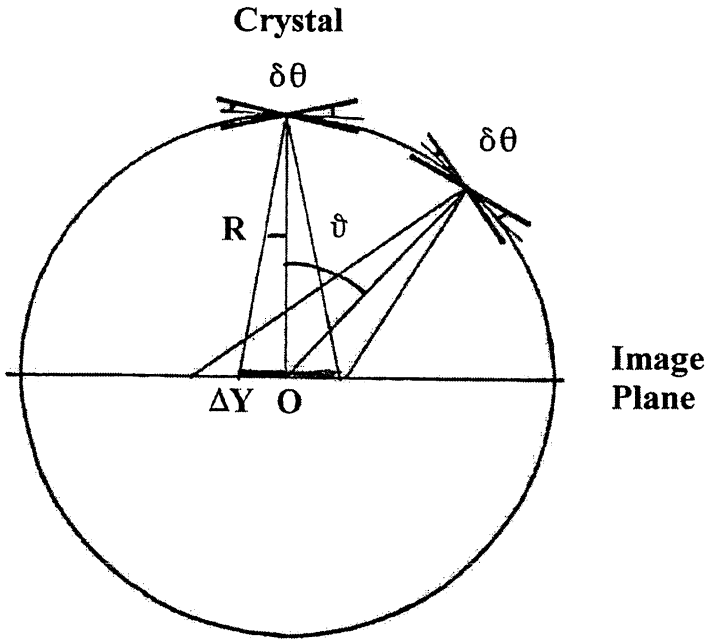


Figure 2. Ray path in a von Hamos spectrometer in a plane perpendicular to the spectrometer axis

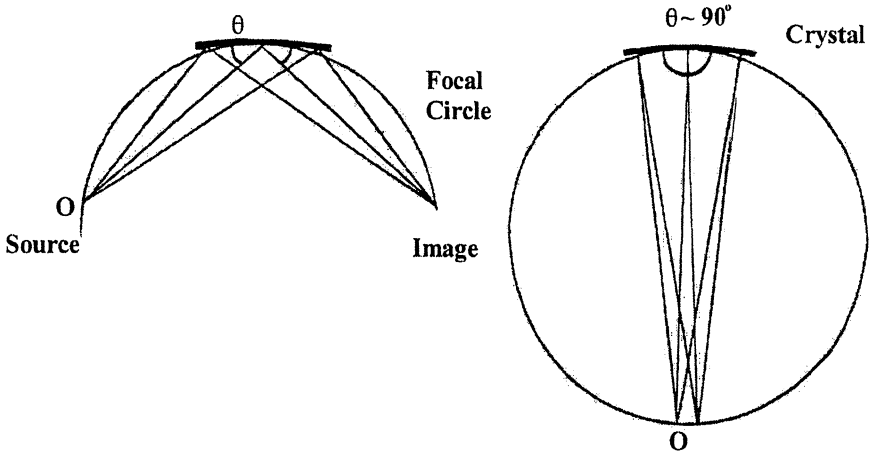


Figure 3. Ray path in a Johann spectrometer

4. EXPERIMENT

A laser-produced plasma was used as an x-ray source to analyze the von Hamos spectrometers. The experiments were performed on the laser-plasma facility at the Lebedev Physical Institute. Plasma was created by focusing the

Downloaded From: http://proceedings.spiedigitallibrary.org/ on 03/27/2014 Terms of Use: http://spiedl.org/terms

Nd glass laser radiation ($0.53\ \mu m/\ 2.5J/2\ ns$) onto a solid Ti target. The laser light flux density on the target was in the order of $\sim 10^{14} W/cm^2$.

Crystals with radius of curvature $R = 20\ mm$ were used in the von Hamos spectrometer. The spectrometer axis was installed perpendicular to the laser beam. Spectra in the vicinity of the resonance line (w) of the [He]-like $TiXX$ ion were recorded on Kodak RAR 2492 x-ray photofilm positioned in the image plane. To prevent visible light illumination, an Al-coated mylar filter ($4.4\ \mu m$ of mylar, $0.2\ \mu m$ of Al) was used. To attenuate x-ray exposure on the photofilm, Al filters of different thicknesses (up to $50\ \mu m$) were used. Spectra were recorded in a single laser shot. Subsequently the spectra were densitometrically traced and converted to relative intensity scales using the table in ref.[7]. Dispersion in the image plane was equal to $D = 0.02324\ \AA/mm$.

Initially, a mica crystal was installed in the spectrometer. The spectrometer was aligned and the spectra were recorded in the third order of mica reflection ($2d = 6.61\AA$). Then a graphite crystal was installed in the same place. The crystal was made from shaped, highly oriented pyrolytic graphite (HOPG)[8] and was mounted on a special cylindrical holder with the same radius of curvature ($R = 20\ mm$). The crystal parameters are: $2d = 6.708\AA$, thickness $\sim 100\ \mu m$ and $\sim 200\ \mu m$, rocking curve FWHM $\sim 0.5°$, peak reflectivity ~ 0.5.

5. EXPERIMENTAL RESULTS AND CONCLUSIONS

Preliminary calibration of the crystals was made using an Fe^{55} isotope source ($\lambda = 2.103\AA$) and a MOXTEK pin diode detector. The measured integrated reflectivities are shown in Table 3. The data are in good agreement with

Table 3. Integrated reflectivity ρ of crystals measured using a Fe^{55} isotope source ($\lambda = 2.103\AA$)

Mica ($20\mu m$ thickness), third-order reflection (effective $2\ d = 19.84/3 = 6.61\ \AA$)	$\rho = 4.06 \cdot 10^{-2} mrad$
Graphite ($100\ \mu m$ thickness), first-order reflection $2\ d = 6.708\ \AA$	$\rho = 125 \cdot 10^{-2} mrad$
Graphite ($200\ \mu m$ thickness), first-order reflection $2\ d = 6.708\ \AA$	$\rho = 278 \cdot 10^{-2} mrad$

ref.[5]. Note that the integrated reflectivity of the graphite crystal is about 30-70 times higher than the mica crystal. The spectrum of titanium laser-produced plasmas obtained with a curved mica (thickness of $20\mu m$) and graphite (thickness of $100\ \mu m$) crystals are shown in Fig. 4. Fig. 4 also shows microdensitometer traces along dispersion (x axis) and transverse to dispersion direction (y axis), i.e., along the spatial resolution direction. In the spectra, several lines are clearly observed: w, y - resonance and intercombination lines of the $[He]$-like $TiXX$ ion; k, j - dielectronic satellites (Gabriel notation[9] for satellite lines is used). From these spectra recorded with different laser pulse energies, the following values were derived:

I_{max} - maximum line intensity;
Δx - FWHM along dispersion;
Δy - FWHM transverse to dispersion;
$I_{int} = I_{max} \cdot \Delta x \cdot \Delta y$ - integral line intensity.

During the spectra analysis, an experimentally obtained relationship for the resonance line (w), $I_{int} \sim E_L^{4.23}$ (E_L - laser pulse energy in J) was used. As a result, the following data were obtained.

Maximum intensity:
I_{max}(graphite)/I_{max}(mica) = 4-6.

Integral intensity:
$I_{int} = I_{max} \cdot \Delta x \cdot \Delta y$:
I_{int}(graphite)/I_{int}(mica) = 60.

Downloaded From: http://proceedings.spiedigitallibrary.org/ on 03/27/2014 Terms of Use: http://spiedl.org/terms

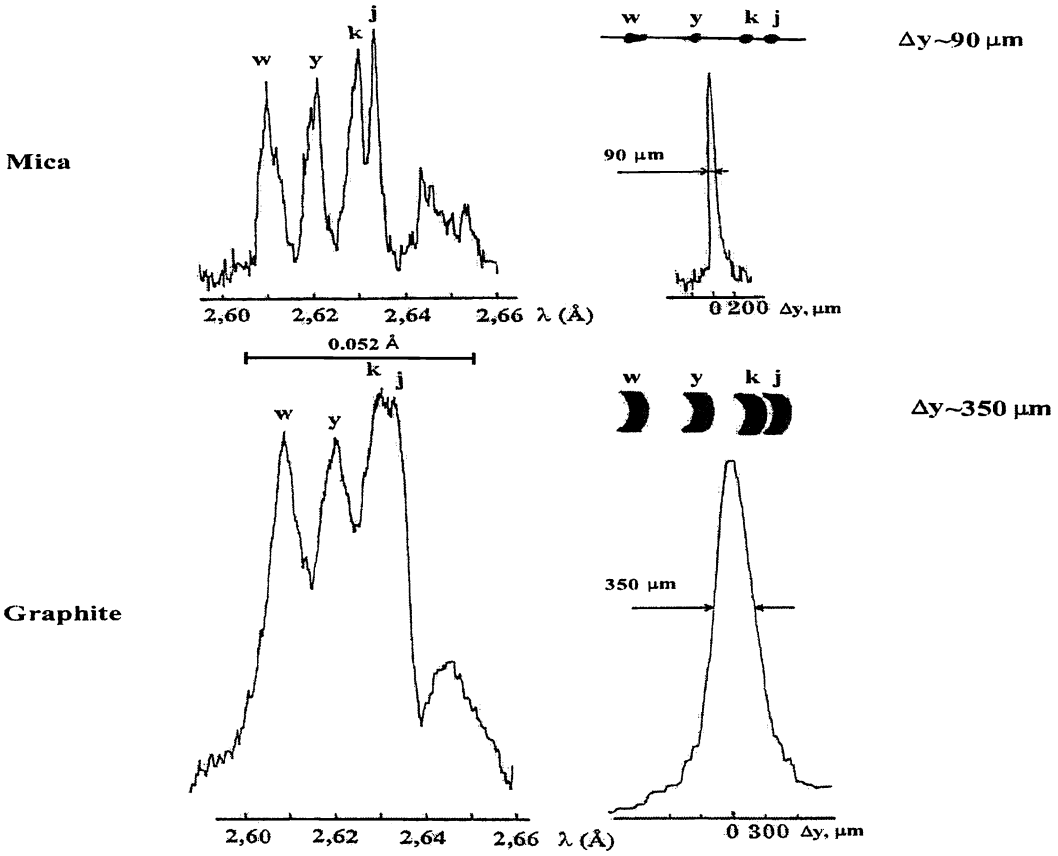


Figure 4. Microdensitometer tracings of Ti spectra

Integral reflectivity:
Using the improved data for mica integrated reflectivity $\rho = (2.1 \pm 0.7) \cdot 10^{-2} mrad$ from ref.[4], we could derive integrated reflectivity for the graphite crystal: $\rho = (130 \pm 40) \cdot 10^{-2} mrad$. This value is in good agreement with our measurements using the isotope source (see Table 3 and ref.[5]).

Spatial resolution:
In ref.[4], it was shown that the mica crystal von Hamos spectrograph has a spatial resolution better than 10 μm. For this reason, the observed value $\Delta y = 90$ μm corresponds to the source size (a). For the graphite spectrograph, the value $\Delta y = 350$ $\mu m \gg a$ - the source size. In this case, the value Δy is defined by the mosaic spread of the crystal (see below): $\Delta y' \sim R \cdot 2 \cdot \delta\theta = 300$ μm for $\delta\theta = 0.5°$ which coincides with the observed value $\Delta y = 350$ μm.

Spectral resolution:
Spectral resolution $\delta\lambda$ was defined from line broadening: $\delta\lambda[\AA] = \Delta x[mm] \cdot D[\AA/mm]$. For the mica crystal, the spectral resolving power was equal to $\lambda/\delta\lambda = 1080$. The appropriate value for the graphite crystal was found to be $\lambda/\delta\lambda = 480$, which is derived from line broadening and $\lambda/\delta\lambda = 764$ derived from resolution of satellites j and k. At the same time, the spectral resolving power defined by the mosaic spread of the graphite crystal gives the value $\lambda/\delta\lambda = \tan\theta/\delta\theta = 50$ for $\delta\theta = 0.5°$. These results are seen visually in Fig. 4, the rocking curve FWHM for mosaic spread is marked by a line segment. Mosaic focusing shows an increase of resolving power by as much as a factor of 10-15.

Downloaded From: http://proceedings.spiedigitallibrary.org/ on 03/27/2014 Terms of Use: http://spiedl.org/terms

In conclusion, we could consider applications of the von Hamos spectrometer with different crystals. When high spatial resolution (up to 10 μm), high spectral resolution ($\lambda/\delta\lambda \geq 1000$) and very wide spectral range (several reflection orders) are needed, it is appropriate to use a von Hamos spectrometer with a mica crystal. This type of spectrometer was successfully used for numerous laser-produced plasmas investigations[4]. The spectrometer is also promising in microbeam x-ray fluorescence analysis. When high efficiency and moderate spectral resolution ($\lambda/\delta\lambda \leq 500$) are desired, use of a von Hamos spectrometer with a graphite crystal is preferable. However in this case, the spectrometer does not have any spatial resolution. It is useful to combine the spectrometer with a CCD linear array as a detector. When the pixel height of the CCD array is equal to Δy, the value defined by the mosaic spread of the crystal (see above), the spectrometer efficiency will be realized to its full extent. Because the graphite crystal has the highest integral reflectivity, the spectrometer will have a maximum possible efficiency for the focusing spectrometer in a wide spectral range. This type of the spectrometer is very promising in x-ray fluorescence analysis and in the x-ray spectroscopy of very low intensity sources.

ACKNOWLEDGMENTS

We thank J. Phillips, P. Moody, G. Stewart, and S. Voronov for technical assistance and helpful discussions. This work was partially supported by MOXTEK, Inc., Orem, Utah.

REFERENCES

1. B. Yaakoby and A. J. Burek, "Crystal Diffraction Systems for X-Ray Spectroscopy, Imaging, and Interferometry of Laser Fusion Targets," *IEEE QE* **19**, pp.1841-1854, 1983.
2. L. v. Hamos "Röntgenspektroskopie und Abbildung mittels gekrúmmter Kristallreflektoren," *Naturwiss* **20**, pp.705-706 1932.
3. Von L. v. Hamos, "Röntgenspektroskopie und Abbildung mittels gekrúmmter Kristallreflektoren", *Ann.Phys* **17**, pp.716-724 1933.
4. A. P. Shevelko, "X-ray spectroscopy of laser-produced plasmas using a von Hamos spectrograph," *SPIE* Vol.3604, pp.91-108, 1998.
5. J. V. Gilfrich, D. B. Brown, and P. G. Burkhalter, "Integral Reflection Coefficient of X-ary Spectrometer Crystals," *Applied Spectroscopy* **29**, pp.322-326, 1975.
6. N. G. Alexandropoulos, G. G. Cohen, "Crystals for Stellar Spectrometers," *Applied Spectroscopy* **28**, pp.155-164, 1975.
7. B. L. Henke, F. G. Fujiwara, M. A. Tester, C. H. Dittmore, and M. A. Palmer, "Low-energy x-ray response of photographic films. II. Experimental characterization," *J. Opt. Soc. Am* **B1**, pp.828-849 1984.
8. A. A. Antonov, V. B. Baryshev, I. G. Grigoryeva, G. N. Kulipanov and N. N. Shchipkov, "Focusing shaped pyrographite monochromators in synchrotron radiation experiments," *Nucl. Instr.and Meth.* **A308**, pp.442-446, 1991.
9. A. H. Gabriel, "Dielectronic satellite spectra for highly charged helium-like ion lines," *Mon. Not. R. Astron. Soc.* **160**, pp. 99-119, 1972.

Downloaded From: http://proceedings.spiedigitallibrary.org/ on 03/27/2014 Terms of Use: http://spiedl.org/terms